

Published in final edited form as:

Brain Struct Funct. 2014 May ; 219(3): 983–994. doi:10.1007/s00429-013-0548-0.

Changes in cerebral morphometry and amplitude of low-frequency fluctuations of BOLD signals during healthy aging: correlation with inhibitory control

Sien Hu¹, Herta H.-A. Chao^{2,3}, Sheng Zhang¹, Jaime S. Ide⁴, and Chiang-shan R. Li^{1,5,6}

¹Department of Psychiatry, Yale University, New Haven, CT 06519

²Department of Internal Medicine, Yale University, New Haven, CT 06519

³Department of Internal Medicine, VA Connecticut Healthcare System, West Haven, CT 06516

⁴Departamento de Ciência e Tecnologia, Universidade Federal de São Paulo, R. Talim, 330, 12231-280, São José dos Campos, SP, Brazil

⁵Department of Neurobiology, Yale University, New Haven, CT 06520

⁶Interdepartmental Neuroscience Program, Yale University, New Haven, CT 06520

Abstract

Aging is known to be associated with changes in cerebral morphometry and in regional activations during resting or cognitive challenges. Here we investigated the effects of age on cerebral gray matter (GM) volumes and fractional amplitude of low-frequency fluctuations (fALFF) of blood oxygenation level dependent (BOLD) signals in 111 healthy adults, 18–72 years of age. GM volumes were computed using voxel-based morphometry as implemented in Statistical Parametric Mapping, and fALFF maps were computed for task-residuals as described in Zhang and Li (2010) for individual participants. Across participants, a simple regression against age was performed for GM volumes and fALFF, respectively, with quantity of recent alcohol use as a covariate. At cluster level $p < 0.05$, corrected for family wise-error of multiple comparisons, GM volumes declined with age in prefrontal/frontal regions, bilateral insula, and left inferior parietal lobule (IPL), suggesting structural vulnerability of these areas to aging. FALFF was negatively correlated with age in the supplementary motor area (SMA), preSMA, anterior cingulate cortex (ACC), bilateral dorsal lateral prefrontal cortex (DLPFC), right IPL, and posterior cingulate cortex (PCC), indicating that spontaneous neural activities in these areas during cognitive performance decrease with age. Notably, these age-related changes overlapped in the prefrontal/frontal regions including the pre-SMA, SMA, and DLPFC. Furthermore, GM volumes and fALFF of the pre-SMA/SMA were negatively correlated with the stop signal reaction time, in accord with our earlier work. Together, these results describe anatomical and functional changes in prefrontal/frontal regions and how these changes are associated with declining inhibitory control during aging.

Keywords

age; aging; morphometry; gray matter volume; amplitude of low-frequency fluctuation (fALFF); spontaneous activity

Introduction

Aging is known to influence cerebral morphometry. Previous studies have reported age-related decrease in gray and white matter volumes, especially in the frontal and parietal areas (Taki et al. 2004; Paul et al. 2005; Chee et al. 2009). Gray matter (GM) volume in the dorsal frontal and inferior parietal regions showed a non-linear decline with age from childhood to late adulthood; in particular, GM volumes in the frontal area declined rapidly and reached a plateau at the age of 60, followed by almost no declines through late adulthood (Sowell et al. 2003). Good et al. (2001) reported GM volume decrease in bilateral insula as well as frontal and parietal regions. Using multivariate pattern analysis that accounted for the interrelationships among brain regions, Su et al. (2012) reported that the precentral and postcentral gyri (see also Seidler et al. 2010), along with the caudate, showed the most volume decline during aging.

The pattern of GM volume change in the aging brain is generally examined using voxel-based morphometry (VBM, Ashburner and Friston 2000). VBM identifies differences in the local composition of brain tissue while discounting large scale differences in gross anatomy and position. The correlation between GM volumes and age informs cerebral morphometrical changes during aging. On the basis of these previous studies, we expect to see age-related decrease of GM volumes predominantly in the frontal and parietal regions.

Age-related changes in cerebral functions can be investigated by using behavioral tasks and contrasting events of interest to target a specific cognitive capacity. For example, a notable observation concerns compensatory activity in older people performing a cognitive task (Reuter-Lorenz and Cappell 2008), which could be accompanied with under-activation in task-related regions (Park et al. 2004). Other studies suggested that older adults use the compensatory mechanism to improve performance only up to a ceiling, when further increase in task difficulty fails to increase brain activations (Nagel et al. 2009, 2011). Our recent work suggests that the psychological construct of the task affects the pattern of activation in the aging brain (Hu et al. 2012); age-related decreases and increases in cerebral activations are each associated with constructs that are dominated by internally and externally driven processes.

An alternative that allows investigators to probe the functional integrity of the entire brain is to make use of low frequency blood oxygenation level dependent (BOLD) signals, which can be derived from the time series collected when participants perform a cognitive task (Zhang and Li 2010, 2012) or are at rest (Margulies et al. 2010; Rosazza and Minati 2011). There is growing evidence that the low-frequency BOLD signals, the “spontaneous” activity, reflect the intrinsic functional connectivity of the brain (Biswal et al. 1995; Fair et al. 2007; Fox and Raichle 2007). The spontaneous fluctuations are present in many neuroanatomical systems, including the motor, visual, auditory, default mode, memory,

language, dorsal and ventral attention systems (Fox and Raichle 2007). Such low-frequency BOLD signals, as reflected in the fractional amplitude of low-frequency fluctuations (fALFF) (Zou et al. 2008; Zhang and Li 2010), may therefore inform task-independent functional changes and complement morphometric analysis of structural changes associated with aging.

In the current study, our aim is to examine to what extent cerebral GM volumes and fALFF show a similar pattern of changes during healthy aging. Our previous work showed that aging is associated with decline in the capacity of inhibitory control, as measured by the stop signal reaction time (SSRT) in the stop signal task (Hu et al. 2012), and that inhibitory control is reflected by the activation of the pre-supplementary motor area (pre-SMA, Li et al. 2006; Chao et al. 2009; Duann et al. 2009). An additional aim is to thus examine whether the structural and functional alterations in the pre-SMA may account for differences in cognitive functioning during aging.

Methods

Participants

One-hundred-and-eleven healthy adults (65 females), between 18 and 72 years of age, participated in this study (Table 1). Participants met the following criteria for inclusion: right-handed and able to read and write English; no current or history of diagnosis of any Axis I psychiatric or substance (except nicotine) use disorders (First et al. 1995); no current use of psychotropic medications; no significant current medical including neurological, cardiovascular, endocrine, renal, hepatic, or thyroid disorders. Women who were pregnant or breast feeding were not recruited. All participants older than 60 years of age were assessed with the Mini Mental State Examination and showed a score above 28 (Folstein et al. 1975). Participants tested negative for cocaine, amphetamines, opioids, and benzodiazepines prior to fMRI. They were further required to be free of MRI-contraindications based on the Yale Magnetic Resonance Research Center's safety guidelines. Participants were assessed for alcohol use in the past year, including the average frequency of drinking and number of drinks per occasion, framed on a monthly basis (Bednarski et al. 2012). All participants signed a written consent after they were given a detailed explanation of the study in accordance with a protocol approved by the Yale Human Investigation Committee.

All participants performed a stop signal task or SST (Logan et al. 1984; Chao et al. 2009; Li et al. 2009; Hu and Li 2011). In the SST, two types of trials, 'GO' and 'STOP' were randomly presented with an inter-trial-interval (ITI) of 2 s (the time between the end of the previous trial and the start of the current trial). A fixation dot appeared on the screen to signal the beginning of each trial. The dot was replaced by a circle – the go signal – after a 'fore-period', which varied from 1 to 5 s (with uniform distribution). The randomized fore-period minimized anticipation and allowed jittering of events of interest. Participants were instructed to press a button on a hand-held button box using the right index finger when they saw the circle. The circle disappeared at button press or after 1 s if the participant failed to respond.

In approximately one quarter of the trials, the circle was followed by a ‘cross’ – the stop signal. Participants were instructed to withhold button press when they saw the stop signal. The trial terminated at button press or after 1 s if the participant successfully inhibited the response. The time between the go and stop signals, the stop signal delay (SSD), started at 200 ms and varied from one stop trial to the next according to a staircase procedure, increasing or decreasing by 67 ms each following a stop success and stop error. With the staircase procedure we anticipated that participants would succeed in withholding the response half of the time.

A critical SSD was computed for each participant that represented the time delay required for the participant to successfully withhold a response in half of the stop trials (Levitt 1971). SSDs across stop trials were grouped into runs (sequences of trials), with each run defined as a monotonically increasing or decreasing series. We derived a mid-run estimate by taking the middle SSD of every second run. The critical SSD was computed by taking the mean of all mid-run SSDs. It was reported that, except for experiments with a small number of trials (less than 30), the mid-run estimate was close to the maximum likelihood estimate of X_{50} (50% SS in the SST, Wetheril et al. 1966). The stop signal reaction time (SSRT) was then computed for each participant by subtracting the critical SSD from the median go trial reaction time (Logan et al. 1984).

Participants were trained briefly on the task before imaging to ensure that they understood the task. They were instructed to quickly press the button when they saw the go signal while keeping in mind that a stop signal might come up in some trials. In the scanner, they completed four 10-minute sessions of the task, with approximately 100 trials in each session.

Imaging protocol and spatial preprocessing of brain images

Conventional T1-weighted spin-echo sagittal anatomical images were acquired for slice localization using a 3T scanner (Siemens Trio). Anatomical images of the functional slice locations were obtained with spin-echo imaging in the axial plan parallel to the Anterior Commissure-Posterior Commissure (AC-PC) line with TR=300 ms, TE=2.5 ms, bandwidth=300 Hz/pixel, flip angle=60°, field of view=220×220 mm, matrix=256×256, 32 slices with slice thickness=4 mm and no gap. A single high-resolution T1-weighted gradient-echo scan was applied on each participant. One hundred and seventy-six slices parallel to the AC-PC line covering the whole brain were acquired with TR=2530ms, TE=3.66ms, bandwidth = 181 Hz/pixel, flip angle = 7°, field of view = 256×256 mm, matrix = 256×256, 1mm³ isotropic voxels. Functional blood oxygenation level dependent (BOLD) signals were then acquired with a single-shot gradient-echo echo-planar imaging (EPI) sequence. Thirty-two axial slices parallel to the AC-PC line covering the whole brain were acquired with TR=2000 ms, TE=25 ms, bandwidth=2004 Hz/pixel, flip angle=85°, field of view=220×220 mm, matrix=64×64, 32 slices with slice thickness=4 mm and no gap. Three hundred images were acquired in each run for a total of 4 runs.

Data were analyzed with Statistical Parametric Mapping (SPM8, Wellcome Department of Imaging Neuroscience, University College London, U.K.). Images from the first five TRs at the beginning of each trial were discarded to enable the signal to achieve steady-state equilibrium between radio frequency pulsing and relaxation.

In the pre-processing of BOLD data, images of each participant were realigned (motion-corrected) and corrected for slice timing. A mean functional image volume was constructed for each participant for each run from the realigned image volumes. These mean images were co-registered with the high resolution structural image and then segmented for normalization to an MNI (Montreal Neurological Institute) EPI template with affine registration followed by nonlinear transformation (Friston et al. 1995; Ashburner and Friston 1999). Finally, images were smoothed with a Gaussian kernel of 8 mm at Full Width at Half Maximum.

Voxel-based morphometry (VBM)

Voxel-based morphometry was performed using the VBM8 toolbox (<http://dbm.neuro.uni-jena.de/vbm/>) packaged in Statistical Parametric Mapping 8 (Wellcome Department of Imaging Neuroscience, University College London, U.K.). T1-images were first co-registered to the Montreal Neurological Institute or MNI template space using a multiple stage affine transformation, during which the 12 parameters were estimated. Co-registration started with a coarse affine registration using mean square differences, followed by a fine affine registration using mutual information. In this step, coefficients of the basis functions that minimize the residual square difference (between individual image and the template) were estimated. After affine transformation, T1-images were corrected for intensity bias field and a local means denoising filter was applied, to account for intensity variations (inhomogeneity) and noise caused by different positions of cranial structures within MRI coil; finally, they were segmented into cerebrospinal fluid, gray and white-matters, using an adaptive maximum a posteriori (MAP) method with k-means initializations, as implemented in VBM8, generating tissue class maps (which included the grey matter or GM maps). Segmented and the initially registered tissue class maps were normalized using Dartel, a fast diffeomorphic image registration algorithm of SPM. As a high-dimensional non-linear spatial normalization method, Dartel generates mathematically consistent inverse spatial transformations. We used the standard customized tissue probability maps (TPM), constructed from 550 healthy subjects to drive the Dartel normalization. Normalized GM maps were modulated to obtain the absolute volume of GM tissue corrected for individual brain sizes. Finally, the GM maps were smoothed by convolving with an isotropic Gaussian kernel. Smoothing helps to compensate for the inexact nature of spatial normalization and reduces the number of statistical comparisons (thus making the correction for multiple comparisons less severe); however, it reduces the accuracy of localization. Most VBM studies used a kernel size of FWHM=12mm. We used a smaller kernel size of FWHM=8mm to achieve localization accuracy.

Fractional amplitude of low-frequency fluctuation (fALFF)

To account for the power spectrum density of the low-frequency fluctuation, Zang et al. (2007) developed an index – the amplitude of low frequency fluctuation (ALFF) – in which the square root of power spectrum was integrated in a low-frequency range in order to examine the regional intensity of spontaneous BOLD fluctuations. Because the ALFF appeared to be sensitive to the physiological noise (Zou et al. 2008), we carried out a fractional ALFF (fALFF) analysis on the task-residual data as in a previous study (Zhang and Li 2010). Briefly, filtered task-residual time series were transformed into the frequency

domain using the fast Fourier transform (FFT). Since the power is proportional to [amplitude]² at a given frequency, the power spectrum obtained by FFT was square rooted to obtain the amplitude. A ratio of the amplitude averaged across 0.009–0.08 Hz to that of the entire frequency range (0–0.25 Hz) was computed at each voxel to obtain the fALFF, creating an amplitude map for the whole brain, which was then normalized: normalized fALFF = (fALFF – global mean fALFF)/standard deviation of global mean.

Previous research suggested that head motions alter BOLD signals and frames with high head motions should be removed in functional connectivity analyses (Power et al. 2012; Van Dijk et al. 2012). Thus, in additional analyses, we removed flagged frames in computing fALFF. In particular, we obtained an index that represents instantaneous head motion, the framewise displacement (FD), computed as the sum of the absolute values of the derivatives of the six realignment parameters. We then removed frames with FD greater than 0.5 in this additional analysis (Power et al. 2012).

Linear correlation with age: GM volume and fALFF

In group analyses, we regressed the GM volumes and fALFF each with age across all participants with recent alcohol use as a covariate. Past research has shown effects of alcohol use on cerebral morphometry, such as volume reduction in the frontal and parietal regions (Jernigan et al. 1991; Kril et al. 1997; Harper 2007). Thus, to reduce possible confounds of alcohol use, we employed the average number of drinks (frequency of drinking × number of drinks per occasion) per month in the previous year as a covariate in the regressions.

Between subject correlation of GM volume and fALFF

In addition to whole brain regression against age, we extracted the GM volume and fALFF by averaging across voxels in each of the 116 brain areas as defined in Automated Anatomical Labeling (AAL) atlas (Tzourio-Mazoyer et al. 2002). We correlated GM volume and fALFF across all participants for each AAL area with linear regressions, and used an alpha of 0.05/116=0.00043 to control for multiple testing.

Results

Behavioral performance

On average, participants responded in 97.7% of the go trials with a median go trial reaction time (goRT) of 657±120ms (mean±SD). They made errors in about half of the stop trials (SS% = 52.5%) and showed a stop signal reaction time (SSRT) of 227±45ms. These results suggested that their overall performance was adequately tracked by the staircase procedure. Of interest here was the age-related change in SSRT ($r=0.3245$, $p=0.0005$, Pearson's regression; Hu et al., 2012). No other performance measures were significantly correlated with age.

Voxel-based morphometry (VBM)

The regression of GM volumes with age across participants showed negative correlation in bilateral insula, putamen, superior and medial frontal gyrus (SFG), bilateral precentral gyri,

left postcentral gyrus, left pre-supplementary motor area (SMA), left inferior parietal lobule (IPL), middle cingulate cortex (MCC), and cerebellum, at $p < .05$ corrected for family-wise error (FWE) (Figure 1; Table 2).

Fractional amplitude of low-frequency fluctuations (fALFF)

The fALFF was negatively correlated with age in inferior and middle temporal gyri (ITG/MTG), pre-SMA extending to the anterior cingulate cortex (ACC) and dorsal lateral prefrontal cortex (DLPFC), posterior cingulate cortex (PCC), MFG, IPL, postcentral gyrus, and cuneus/precuneus (cluster $p < .05$ corrected for FWE) (Figure 2; Table 3). In additional analyses we removed image frames with excessive head motions before regressions. The results showed a negative correlation with fALFF in largely identical structures (Supplementary Figure 1).

Between subject correlation of GM volume and fALFF

In between-subject correlations of GM volume and fALFF, five of the 116 AAL areas showed a significant correlation after Bonferroni correction ($p = .05/116 = 0.00043$): bilateral pre-SMA/SMA ($r_{\text{Left}} = 0.3527$, $p_{\text{Left}} = 0.0001$, $r_{\text{Right}} = 0.3749$, $p_{\text{Right}} = 0.0001$), mid cingular cortex (MCC) ($r_{\text{Left}} = 0.4497$, $p_{\text{Left}} = 0.0000$, $r_{\text{Right}} = 0.4367$, $p_{\text{Right}} = 0.0000$), and the right caudate ($r = 0.3358$, $p = 0.0003$).

Alternative analyses: comparison between middle and old age groups

In addition to simple regression against age, we also examined specifically differences between the middle and old age groups. We combined individuals between 30 and 49 years of age as the middle age group and those 50 years or over as the old age group, and conducted a two sample t test on group difference for all of the regions of interest as well as individual regions each for GM volume and fALFF. These results are presented in the Supplement (Supplementary Figures 2, 3, and 4).

Areas showing overlapping changes in GM volume and fALFF

Our between-subject ALL mask-based analyses suggested that, while the great majority of brain regions did not show correlations between GM volume and fALFF, a few areas showed such correlations, including the bilateral pre-SMA/SMA, mid-cingulate cortex (MCC), and the right caudate. We thus examined whether these regions could also be captured by voxel-wise age regressions conducted separately for GM volume and fALFF. We performed an intersection or inclusion operation of the GM (Figure 1) and fALFF (Figure 2) maps using MarsBar. Figure 3 shows areas that overlapped between the two regressions, which included two clusters in the pre-SMA/SMA (anterior pre-SMA and posterior pre-SMA extending to SMA), and a few smaller clusters in the MCC, bilateral DLPFC, and bilateral MFG. As expected, the GM volume and fALFF of the preSMA/SMA (combinations of the two clusters) was significantly correlated across participants ($r = 0.3906$, $p = 0.0000$).

Correlations with stop signal reaction time

To examine the relationship between structural/functional changes and cognitive functions in aging, we correlated the stop signal reaction time (SSRT) with the GM volume and fALFF of all overlapping regions. Results showed that SSRT was significantly correlated with the anterior pre-SMA in GM volume ($r=-0.2671$, $p=0.0046$), after Bonferroni correction ($p=.05/7=.0071$); it was also significantly correlated with the fALFF of posterior pre-SMA extending to SMA ($r=-0.3251$, $p=0.0005$) and the combination of the two clusters of pre-SMA/SMA ($r=-0.2953$, $p=0.0017$) (Figure 4). SSRT was not significantly correlated with the GM volume or fALFF of any other areas.

Discussion

Structural brain correlates of aging: Gray matter volumes

Our results showed that aging is associated with decreased gray matter (GM) volume in frontal and parietal lobes, including the pre-supplementary motor area (SMA), SMA, anterior cingulate cortex (ACC), dorsal lateral prefrontal cortex (DLPFC), and inferior parietal lobule (IPL), as well as bilateral insula, putamen, and postcentral gyrus. These results are consistent with the idea that the frontal and parietal regions are most vulnerable to aging (Sowell et al. 2003), as well as age-related decline in GM volumes of sensorimotor and subcortical regions (Good et al. 2001; Su et al. 2012).

The decrement of GM volume, especially in the frontal regions, begins in early adulthood and continues through the life span. In a study of two cohorts of participants with a wide age range, Bergfield et al. (2010) reported a consistent pattern of changes in GM volume in association with healthy aging. This network includes the bilateral medial frontal cortices (including pre-SMA and SMA), insula/perisylvian cortex, and ACC. Additionally, GM volumes in bilateral DLPFC, IPL, and caudate were also found to decrease with aging. Giorgio et al. (2010) found age-associated GM volume reduction in extensive areas including the superior/middle frontal gyri (including SMA, preSMA, and DLPFC) and postcentral gyrus, in addition to subcortical structures such as the caudate nucleus, pallidum, and hippocampus. Taki et al. (2011) observed a significant GM volume deduction with age in the precentral gyrus, postcentral gyrus, middle frontal gyrus, and insula (also in Good et al. 2001; Grieve et al. 2005) as well as in mid and posterior cingulate cortices (Taki et al. 2012). It was shown that the limbic system including the mid-cingulate cortex (MCC) declines rapidly from childhood to early adulthood and remains steady in volume afterwards (Grieve et al. 2005). Thus, the observation of a negative correlation of MCC volume with age appears to reflect a greater number of participants in their early adulthood in the current study. In sum, the current results are consistent with a large body of aging morphometrics literature, with the notable exception of the hippocampus.

Hippocampus is critical to memory function, which declines in the elderly. There is discrepancy as to the effect of age on hippocampal structures; some studies reported a prominent age effect (Raz et al. 2005; Giorgio et al. 2010), while others did not (Good et al. 2001; Grieve et al. 2005; Folstein and Folstein 2010). There are a few possible explanations for this inconsistency. First, the volume of hippocampus increases until the age of 40 and

starts to decrease afterwards, with a speeded decline after the age of 50 (Long et al. 2012). In our sample, 76% of our participants were under age 40 and only 1 participant was over 70. Thus, our cohort may not have an adequate age range to capture age related changes in hippocampal volumes. Second, GM volume reduction in the hippocampus is associated with memory decline (Kramer et al. 2007), as occurs in people with amnesic mild cognitive impairment or Alzheimer's disease (Kantarci and Jack 2003; Fellgiebel and Yakushev 2011). Folstein & Folstein (2010) compared the hippocampal volume in two elderly cohorts and observed hippocampal volume decrement in dementia patients but not in healthy controls. Our older participants in the current study appeared to be intact in their cognitive status, as assessed by MMSE, and thus may not show changes in hippocampal volumes. Third, and more broadly, one could consider the differences between longitudinal and cross-sectional studies. Longitudinal studies (e.g., Raz et al. 2005) focus on within-subject comparisons and might be more sensitive than cross-sectional studies (e.g., Good et al. 2001; Grieve et al. 2005), where between-subject variability introduces additional noise, in picking up changes in cerebral volumes.

Functional brain correlates of aging: fALFF

The fractional amplitude of low-frequency fluctuation (fALFF) is negatively correlated with age in the posterior cingulate cortex (PCC), ACC, pre-SMA, DLPFC, IPL, and middle temporal gyrus (MTG). This result is consistent with Biswal (Biswal et al. 2010) where they reported age-related decreased fALFF in the posterior cingulate cortex. In addition, previous research on functional connectivity also reported that whole-brain connectivity in the PCC decreases as age increases (Littow et al. 2010; Jones et al. 2011). The anterior frontal network is involved in many cognitive functions including attention, execution control, and speed of information processing (Buckner 2004; Eckert 2011). It is plausible that the age-related decrement of the intrinsic activity in the anterior frontal network reflects a general decline of cognitive ability during aging, as we also observed for the stop signal reaction time (SSRT, see below). To our knowledge, there have been only a few studies on the effects of age on changes in the amplitude of low-frequency fluctuation of BOLD signals. Reduced ALFF in the visual cortex was observed in older compared to younger adults during visual checkerboard stimulation (Yan et al. 2011). Patients with mild cognitive impairment (MCI) showed decreased ALFF/fALFF in prefrontal and left parietal regions, compared to age-matched healthy participants (Han et al. 2012), and recent studies have suggested the importance in assessing executive dysfunction in addition to memory impairment in individuals with MCI (Morris 2012). Our results add to these earlier studies by showing age-related decrease in fALFF in multiple cortical and subcortical structures.

Correlation of anatomical and functional changes in aging

The effects of age on structural and functional changes are each shown in the regression of GM volume and fALFF with age. A notable finding is that areas including the pre-SMA/SMA, MCC, bilateral DLPFC, and bilateral MFG showed significant negative correlation with age in both regressions (Figure 3), suggesting a concurrent change in structure and function during aging. On the other hand, the majority of brain regions do not demonstrate a similar age effect in the changes of GM volume and fALFF. In a recent work, Han et al. compared the GM volumes and ALFF/fALFF between patients with amnesic MCI and age-

matched healthy controls (2012). The patient group showed decreased GM volumes in bilateral prefrontal and PCC areas, and decreased ALFF/fALFF in prefrontal and left parietal areas. These investigators concluded that it is essential to examine both anatomical and functional changes as they complement each other in our understanding of the effects of aging on the brain. Our current results support this idea but also highlight an intriguing possibility that prefrontal brain regions, especially those that are critical for executive functions, show concurrent age-related changes in structure and function.

Age-related correlates of the decline in inhibitory control

A second goal of this study is to examine whether the structural and functional alterations accounts for differences in stop signal performance during aging. Results revealed a negative correlation between SSRT and the GM volume of pre-SMA, consistent with the finding that age-related changes in different cerebral regions especially in the frontal network affect processing speed (Eckert 2011). More generally, aging is associated with declining processing speed across multiple cognitive domains, including sensory-motor mapping and high-level executive mechanisms, and structural changes in medial frontal (including pre-SMA) and lateral frontal cortices. Our previous work suggested that higher task-evoked BOLD signals of the pre-SMA is associated with a greater capacity in inhibitory control (Li et al. 2006; Chao et al. 2009; Duann et al. 2009), and that such capacity declined significantly with age (Hu et al. 2012). Therefore, the significant correlation between SSRT and the GM volume/fALFF of the pre-SMA/SMA further underscores the importance of this medial prefrontal region in age-associated changes in inhibitory control.

Limitations of the study

An important limitation of the study is that our cohort contained only 8 participants older than 60 years of age. Thus, although the findings address the effects of age on GM volume and fALFF, they may not capture the changes that are most prominent in the elderly population. Second, physiological noises such as those resulting from respiration and heart beat are known to affect low frequency BOLD signals (Birn et al., 2008; Chang & Glover, 2009; Chang, Cunningham, & Glover, 2009). Since we did not collect respiratory and cardiovascular data, we do not know how much the current results are influenced by these physiological noises. On the other hand, the brain areas that are mostly affected by the physiological noise appear to be those in the default mode network (Birn et al., 2006), while our main findings of the effects of age on GM volume and fALFF are in the prefrontal regions. With these caveats, the current findings need to be replicated in future work.

Conclusions

The current study explored the relationship between the anatomical and functional changes during healthy aging. We found that age-related decrement in GM volumes and low-frequency BOLD signals overlaps in the frontal brain areas. The structural and functional alterations in the pre-SMA are associated with the decline in response inhibition associated with aging.

Supplementary Material

Refer to Web version on PubMed Central for supplementary material.

Acknowledgments

This study was supported by NIH grant K02DA026990 (Li), a Yale Cancer Center grant for translational pilot study (Chao), and the William O. Seery Foundation (Chao). We thank Dr. Dianne Lee, Olivia Farr, Sarah Bednarski, and Emily Erdman for their many helpful discussions.

References

- Ashburner J, Friston KJ. Nonlinear spatial normalization using basis functions. *Hum Brain Mapp.* 1999; 7:254–266. [PubMed: 10408769]
- Ashburner J, Friston KJ. Voxel-based morphometry - The methods. *Neuroimage.* 2000; 11:805–821. [PubMed: 10860804]
- Bednarski SR, Erdman E, Luo X, Zhang S, Hu S, Li CS. Neural Processes of an Indirect Analog of Risk Taking in Young Nondependent Adult Alcohol Drinkers-An fMRI Study of the Stop Signal Task. *Alcohol Clin Exp Res.* 2012; 36:768–779. [PubMed: 22339607]
- Bergfield KL, Hanson KD, Chen KW, Teipel SJ, Hampel H, Rapoport SI, Moeller JR, Alexander GE. Age-related networks of regional covariance in MRI gray matter: Reproducible multivariate patterns in healthy aging. *Neuroimage.* 2010; 49:1750–1759. [PubMed: 19796692]
- Birn RM, Diamond JB, Smith MA, Bandettini PA. Separating respiratory-variation-related neuronal-activity-related fluctuations in fluctuations from fMRI. *Neuroimage.* 2006; 31:1536–1548. [PubMed: 16632379]
- Birn RM, Smith MA, Jones TB, Bandettini PA. The respiration response function: the temporal dynamics of fMRI signal fluctuations related to changes in respiration. *Neuroimage.* 2008; 40:644–654. [PubMed: 18234517]
- Biswal B, Yetkin FZ, Haughton VM, Hyde JS. Functional Connectivity in the Motor Cortex of Resting Human Brain Using Echo-Planar Mri. *Magnet Reson Med.* 1995; 34:537–541.
- Biswal BB, Mennes M, Zuo XN, Gohel S, Kelly C, Smith SM, Beckmann CF, Adelstein JS, Buckner RL, Colcombe S, Dogonowski AM, Ernst M, Fair D, Hampson M, Hoptman MJ, Hyde JS, Kiviniemi VJ, Kotter R, Li SJ, Lin CP, Lowe MJ, Mackay C, Madden DJ, Madsen KH, Margulies DS, Mayberg HS, McMahon K, Monk CS, Mostofsky SH, Nagel BJ, Pekar JJ, Peltier SJ, Petersen SE, Riedl V, Rombouts SARB, Rypma B, Schlaggar BL, Schmidt S, Seidler RD, Siegle GJ, Sorg C, Teng GJ, Veijola J, Villringer A, Walter M, Wang LH, Weng XC, Whitfield-Gabrieli S, Williamson P, Windischberger C, Zang YF, Zhang HY, Castellanos FX, Milham MP. Toward discovery science of human brain function. *P Natl Acad Sci USA.* 2010; 107:4734–4739.
- Buckner RL. Memory and executive function in aging and AD: multiple factors that cause decline and reserve factors that compensate. *Neuron.* 2004; 44:195–208. [PubMed: 15450170]
- Chang C, Cunningham JP, Glover GH. Influence of heart rate on the BOLD signal: The cardiac response function. *Neuroimage.* 2009; 44:857–869. [PubMed: 18951982]
- Chang C, Glover GH. Relationship between respiration, end-tidal CO₂, and BOLD signals in resting-state fMRI. *Neuroimage.* 2009; 47:1381–1393. [PubMed: 19393322]
- Chao HH, Luo X, Chang JL, Li CS. Activation of the pre-supplementary motor area but not inferior prefrontal cortex in association with short stop signal reaction time – an intra-subject analysis. *BMC Neurosci.* 2009; 10:75. [PubMed: 19602259]
- Chee MWL, Chen KHM, Zheng H, Chan KPL, Isaac V, Sim SKY, Chuah LYM, Schuchinsky M, Fischl B, Ng TP. Cognitive function and brain structure correlations in healthy elderly East Asians. *Neuroimage.* 2009; 46:257–269. [PubMed: 19457386]
- Duann JR, Ide JS, Luo X, Li CS. Functional connectivity delineates distinct roles of the inferior frontal cortex and presupplementary motor area in stop signal inhibition. *J Neurosci.* 2009; 29:10171–10179. [PubMed: 19675251]

- Eckert MA. Slowing down: age-related neurobiological predictors of processing speed. *Front Neurosci.* 2011; 5:25. [PubMed: 21441995]
- Fair DA, Schlaggar BL, Cohen AL, Miezin FM, Dosenbach NUF, Wenger KK, Fox MD, Snyder AZ, Raichle ME, Petersen SE. A method for using blocked and event-related fMRI data to study “resting state” functional connectivity. *Neuroimage.* 2007; 35:396–405. [PubMed: 17239622]
- Fellgiebel A, Yakushev I. Diffusion Tensor Imaging of the Hippocampus in MCI and Early Alzheimer’s Disease. *J Alzheimers Dis.* 2011; 26:257–262. [PubMed: 21971465]
- First, M.; Spitzer, R.; Williams, JMG. Structured clinical interview for DSM-IV (SCID). American Psychiatric Association; Washington DC: 1995.
- Folstein M, Folstein S. Functional expressions of the aging brain. *Nutr Rev.* 2010; 68(Suppl 2):S70–73. [PubMed: 21091951]
- Folstein MF, Folstein SE, McHugh PR. Mini-Mental State - Practical Method for Grading Cognitive State of Patients for Clinician. *J Psychiat Res.* 1975; 12:189–198. [PubMed: 1202204]
- Fox MD, Raichle ME. Spontaneous fluctuations in brain activity observed with functional magnetic resonance imaging. *Nat Rev Neurosci.* 2007; 8:700–711. [PubMed: 17704812]
- Friston K, Holmes AP, Worsley KJ, Poline JB, Frith CD, Frackowiak R. Statistical parametric maps in functional imaging: a general linear approach. *Hum Brain Mapp.* 1995; 2:189–210.
- Giorgio A, Santelli L, Tomassini V, Bosnell R, Smith S, De Stefano N, Johansen-Berg H. Age-related changes in grey and white matter structure throughout adulthood. *Neuroimage.* 2010; 51:943–951. [PubMed: 20211265]
- Good CD, Johnsrude IS, Ashburner J, Henson RNA, Friston KJ, Frackowiak RSJ. A voxel-based morphometric study of ageing in 465 normal adult human brains. *Neuroimage.* 2001; 14:21–36. [PubMed: 11525331]
- Grieve SM, Clark CR, Williams LM, Peduto AJ, Gordon E. Preservation of limbic and paralimbic structures in aging. *Hum Brain Mapp.* 2005; 25:391–401. [PubMed: 15852381]
- Han Y, Lui S, Kuang W, Lang Q, Zou L, Jia J. Anatomical and functional deficits in patients with amnesic mild cognitive impairment. *Plos One.* 2012; 7:e28664. [PubMed: 22319555]
- Harper C. The neurotoxicity of alcohol. *Hum Exp Toxicol.* 2007; 26:251–257. [PubMed: 17439928]
- Hu S, Chao HH, Winkler AD, Li CS. The effects of age on cerebral activations: internally versus externally driven processes. *Front Aging Neurosci.* 2012; 4:4. [PubMed: 22536185]
- Hu S, Li CS. Neural processes of preparatory control for stop signal inhibition. *Hum Brain Mapp.* 2011 [Epub ahead of print]. 10.1002/hbm.21399
- Jernigan TL, Butters N, Ditraglia G, Schafer K, Smith T, Riwin M, Grant I, Schuckit M, Cermak LS. Reduced Cerebral Gray-Matter Observed in Alcoholics Using Magnetic-Resonance-Imaging. *Alcohol Clin Exp Res.* 1991; 15:418–427. [PubMed: 1877728]
- Jones DT, Machulda MM, Vemuri P, McDade EM, Zeng G, Senjem ML, Gunter JL, Przybelski SA, Avula RT, Knopman DS, Boeve BF, Petersen RC, Jack CR. Age-related changes in the default mode network are more advanced in Alzheimer disease. *Neurology.* 2011; 77:1524–1531. [PubMed: 21975202]
- Kantarci K, Jack CR. Neuroimaging in Alzheimer disease: An evidence-based review. *Neuroimag Clin N Am.* 2003; 13:197–203.
- Kramer JH, Mungas D, Reed BR, Wetzel ME, Burnett MM, Chui HC, Miller BL, Weiner MW. Longitudinal MRI and cognitive change in healthy elderly. *Neuropsychology.* 2007; 21:412–418. [PubMed: 17605574]
- Kril JJ, Halliday GM, Svoboda MD, Cartwright H. The cerebral cortex is damaged in chronic alcoholics. *Neuroscience.* 1997; 79:983–998. [PubMed: 9219961]
- Levitt H. Transformed up-down Methods in Psychoacoustics. *J Acoust Soc Am.* 1971; 49:467–477. [PubMed: 5541744]
- Li CSR, Chao HHA, Lee TW. Neural Correlates of Speeded as Compared with Delayed Responses in a Stop Signal Task: An Indirect Analog of Risk Taking and Association with an Anxiety Trait. *Cereb Cortex.* 2009; 19:839–848. [PubMed: 18678764]

- Li CSR, Huang C, Constable RT, Sinha R. Imaging response inhibition in a stop-signal task: neural correlates independent of signal monitoring and post-response processing. *J Neurosci*. 2006; 26:186–192. [PubMed: 16399686]
- Littow H, Elseound AA, Haaepa M, Isohanni M, et al. Age-related differences in functional nodes of the brain cortex - a high model order group ICA study. *Front Sys Neuroisci*. 2010; 4:32.
- Logan GD, Cowan WB, Davis KA. On the Ability to Inhibit Simple and Choice Reaction-Time Responses – a Model and a Method. *J Exp Psychol Hum Percept Perform*. 1984; 10:276–291. [PubMed: 6232345]
- Long X, Liao W, Jiang C, Liang D, Qiu B, Zhang L. Healthy aging: an automatic analysis of global and regional morphological alterations of human brain. *Acad Radiol*. 2012; 19:785–793. [PubMed: 22503890]
- Margulies DS, Böttger J, Long XY, Lv YT, Kelly C, Schafer A, Goldhahn D, Abbushi A, Milham MP, Lohmann G, Villringer A. Resting developments: a review of fMRI post-processing methodologies for spontaneous brain activity. *Magn Reson Mater Phy*. 2010; 23:289–307.
- Morris JC. Revised Criteria for Mild Cognitive Impairment May Compromise the Diagnosis of Alzheimer Disease Dementia. *Arch Neurol*. 2012; 69(6):700–708. [PubMed: 22312163]
- Nagel IE, Preuschhof C, Li SC, Nyberg L, Backman L, Lindenberger U, Heekeren HR. Performance level modulates adult age differences in brain activation during spatial working memory. *P Natl Acad Sci USA*. 2009; 106:22552–22557.
- Nagel IE, Preuschhof C, Li SC, Nyberg L, Backman L, Lindenberger U, Heekeren HR. Load Modulation of BOLD Response and Connectivity Predicts Working Memory Performance in Younger and Older Adults. *J Cognitive Neurosci*. 2011; 23:2030–2045.
- Park DC, Polk TA, Park R, Minear M, Savage A, Smith MR. Aging reduces neural specialization in ventral visual cortex. *P Natl Acad Sci USA*. 2004; 101:13091–13095.
- Paul RH, Haque O, Gunstad J, Tate DF, Grieve SM, Hoth K, Brickman AM, Cohen R, Lange K, Jefferson AL, MacGregor KL, Gordon E. Subcortical hyperintensities impact cognitive function among a select subset of healthy elderly. *Arch Clin Neuropsych*. 2005; 20:697–704.
- Power JD, Barnes KA, Snyder AZ, Schlaggar BL, Petersen SE. Spurious but systematic correlations in functional connectivity MRI networks arise from subject motion. *Neuroimage*. 2012; 59:2142–2154. [PubMed: 22019881]
- Raz N, Lindenberger U, Rodrigue KM, Kennedy KM, Head D, Williamson A, Dahle C, Gerstorf D, Acker JD. Regional brain changes in aging healthy adults: general trends, individual differences and modifiers. *Cereb Cortex*. 2005; 15:1676–1689. [PubMed: 15703252]
- Reuter-Lorenz PA, Cappell KA. Neurocognitive aging and the compensation hypothesis. *Curr Dir Psychol Sci*. 2008; 17:177–182.
- Rosazza C, Minati L. Resting-state brain networks: literature review and clinical applications. *Neuro Sci*. 2011; 32:773–785. [PubMed: 21667095]
- Seidler RD, Bernard JA, Burutolu TB, Fling BW, Gordon MT, Gwin JT, Kwak Y, Lipps DB. Motor control and aging: Links to age-related brain structural, functional, and biochemical effects. *Neurosci Biobehav R*. 2010; 34:721–733.
- Sowell ER, Peterson BS, Thompson PM, Welcome SE, Henkenius AL, Toga AW. Mapping cortical change across the human life span. *Nat Neurosci*. 2003; 6:309–315. [PubMed: 12548289]
- Su L, Wang L, Chen F, Shen H, Li B, Hu D. Sparse representation of brain aging: extracting covariance patterns from structural MRI. *Plos One*. 2012; 7:e36147. [PubMed: 22590522]
- Taki Y, Goto R, Evans A, Zijdenbos A, Neelin P, Lerch J, Sato K, Ono S, Kinomura S, Nakagawa M, Sugiura M, Watanabe J, Kawashima R, Fukuda H. Voxel-based morphometry of human brain with age and cerebrovascular risk factors. *Neurobiol Aging*. 2004; 25:455–463. [PubMed: 15013566]
- Taki Y, Hashizume H, Thyreau B, Sassa Y, Takeuchi H, Wu K, Kotozaki Y, Nouchi R, Asano M, Asano K, Fukuda H, Kawashima R. Linear and curvilinear correlations of brain gray matter volume and density with age using voxel-based morphometry with the Akaike information criterion in 291 healthy children. *Hum Brain Mapp*. 2012 [Epub ahead of print]. 10.1002/hbm.22033

- Taki Y, Thyreau B, Kinomura S, Sato K, Goto R, Kawashima R, Fukuda H. Correlations among Brain Gray Matter Volumes, Age, Gender, and Hemisphere in Healthy Individuals. *Plos One*. 2011; 6:e22734. [PubMed: 21818377]
- Tzourio-Mazoyer N, Landeau B, Papathanassiou D, Crivello F, Etard O, Delcroix N, Mazoyer B, Joliot M. Automated anatomical labeling of activations in SPM using a macroscopic anatomical parcellation of the MNI MRI single-subject brain. *Neuroimage*. 2002; 15:273–289. [PubMed: 11771995]
- Van Dijk KRA, Sabuncu MR, Buckner RL. The influence of head motion on intrinsic functional connectivity MRI. *Neuroimage*. 2012; 59:431–438. [PubMed: 21810475]
- Wetheril GB, Chen H, Vasudeva RB. Sequential Estimation of Quantal Response Curves – a New Method of Estimation. *Biometrika*. 1966; 53:439–454.
- Yan L, Zhuo Y, Wang B, Wang DJ. Loss of Coherence of Low Frequency Fluctuations of BOLD FMRI in Visual Cortex of Healthy Aged Subjects. *Open Neuroimag J*. 2011; 5:105–111. [PubMed: 22216081]
- Zang YF, He Y, Zhu CZ, Cao QJ, Sui MQ, Liang M, Tian LX, Jiang TZ, Wang YF. Altered baseline brain activity in children with ADHD revealed by resting-state functional MRI. *Brain Dev*. 2007; 29:83–91. [PubMed: 16919409]
- Zhang S, Li CS. A neural measure of behavioral engagement: task-residual low-frequency blood oxygenation level-dependent activity in the precuneus. *Neuroimage*. 2010; 49:1911–1918. [PubMed: 19761851]
- Zhang S, Li CS. Task-related, low-frequency task-residual, and resting state activity in the default mode network brain regions. *Front Psychol*. 2012; 3:172. [PubMed: 22661964]
- Zou QH, Zhu CZ, Yang YH, Zuo XN, Long XY, Cao QJ, Wang YF, Zang YF. An improved approach to detection of amplitude of low-frequency fluctuation (ALFF) for resting-state fMRI: Fractional ALFF. *J Neurosci Meth*. 2008; 172:137–141.

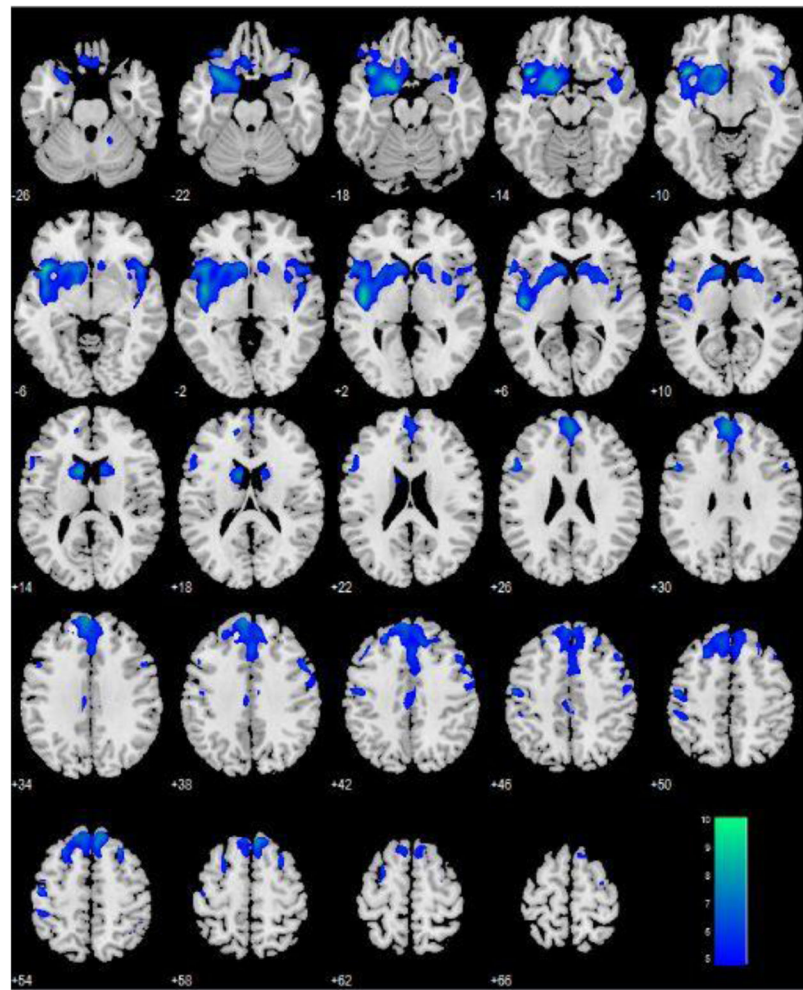


Figure 1.

Decrement of gray matter (GM) volume with aging, with the quantity of recent drinking accounted for in a linear regression. Areas include bilateral insula, putamen, pre-supplementary motor area (SMA) / SMA, mid cingulate cortex, right middle frontal gyrus, left precentral gyrus, and left inferior parietal lobule. All clusters survived at $p < .05$ corrected for family-wise error (FWE) of multiple comparisons. Color bar represents voxel T value.

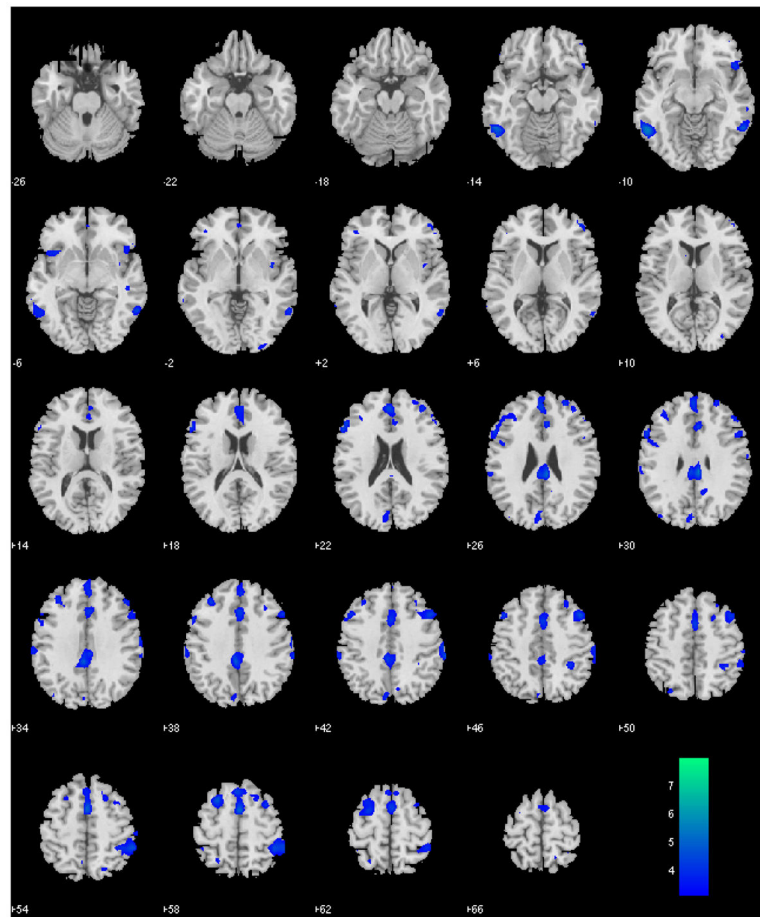


Figure 2.

Brain regions with age-related decrease in the fractional amplitude of low-frequency fluctuations (fALFF), controlling for the quantity of recent drinking. Areas include the bilateral inferior and middle temporal gyri, pre-supplementary motor area extending to anterior cingulate cortex and dorsal lateral prefrontal cortex, post cingulate cortex, left middle frontal gyrus, right inferior parietal lobule, left postcentral gyrus, and bilateral cuneus/precuneus. All clusters survived at $p < .05$ corrected for family-wise error (FWE) of multiple comparisons. Color bar represents voxel T value.

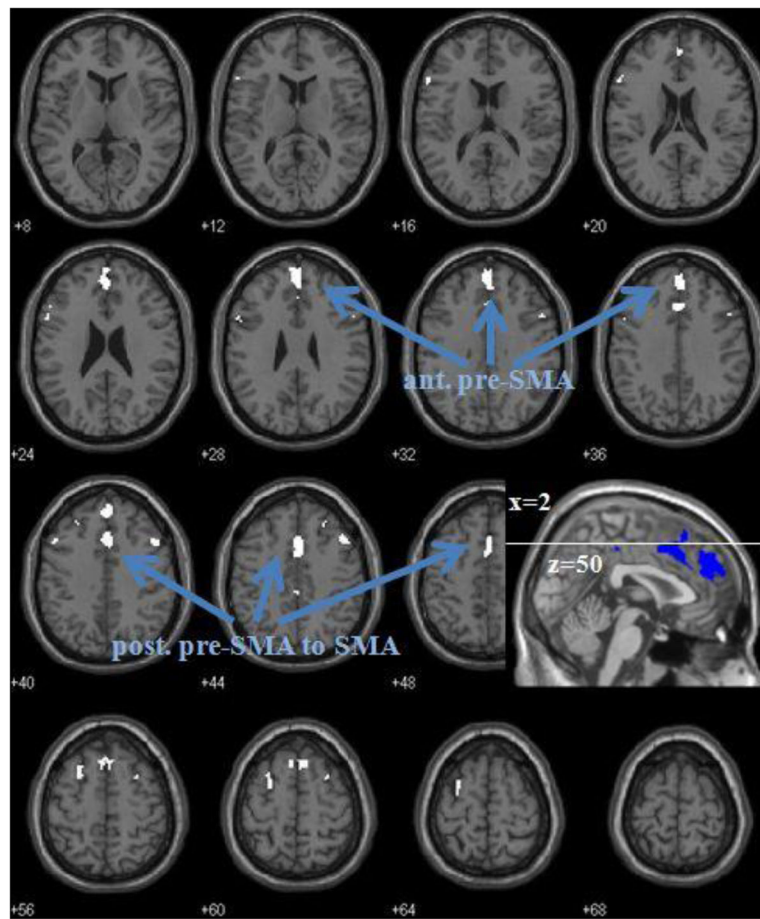


Figure 3.

Areas overlapped in the regression of age with GM volumes and with fALFF, including the anterior pre-supplementary motor area (SMA) and posterior pre-SMA extending to SMA, bilateral dorsal lateral prefrontal cortices, bilateral middle frontal gyri, and mid cingulate cortex. All clusters survived at $p < .05$ corrected for family-wise error (FWE) of multiple comparisons. The inset shows the two clusters (blue), anterior pre-SMA and posterior pre-SMA/SMA, in a sagittal section at $x=2$.

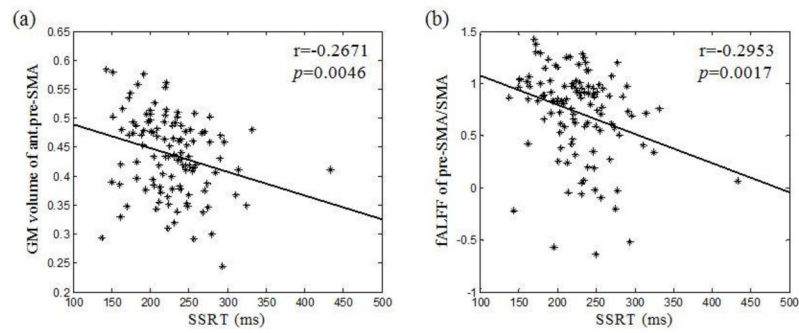


Figure 4.

Negative correlation of SSRT with (a) the GM volume of anterior pre-supplementary motor area (SMA), and (b) the fALFF of the combination of two clusters in the pre-SMA/SMA. Each data point represents one subject.

Table 1

The number of subjects broken down by age and gender.

Age	All	Men	Women
18–19	3	3	0
20–29	63	20	43
30–39	18	8	10
40–49	8	4	4
50–59	11	7	4
60–69	7	4	3
≥70	1	0	1

Table 2

Areas of gray matter (GM) volume negatively correlated with age, with the quantity of recent drinking as a covariate.

Side	Region	Cluster Size	Z Value	MINI Coordinate		
				X	Y	Z
L	Insula	13,512	Inf	-42	16	-8
L/R	pre-SMA/SMA	8,482	7.01	-3	55	32
R	Insula	3,857	6.73	46	15	-7
L	Postcentral G	500	6.56	-50	-14	52
R	Precentral G	744	6.51	52	12	37
L	IPL	213	5.48	-45	-38	52
L/R	MCC	379	5.11	-3	-21	41
L	pre-SMA	66	5.06	-8	3	71
R	MFG	24	4.96	30	-8	65
L	Precentral G	11	4.84	-45	-5	53
R	Cerebellum	77	4.79	28	-53	-34

Note: SMA: supplemental motor area; IPL: inferior parietal lobule; MCC: mid cingulate cortex; MFG: middle frontal gyrus. G: gyrus.

Table 3

Areas of fractional amplitude of low-frequency fluctuations (fALFF) negatively correlated with age, with the quantity of recent drinking as a covariate.

Side	Region	Cluster Size	Z Value	MNI Coordinate		
				X	Y	Z
L	ITG	107	5.69	-57	-52	-11
L/R	pre-SMA/ACC/DLPFC	867	5.18	0	5	55
L/R	PCC	155	5.15	-3	-37	37
L	MFG	116	5.04	-24	14	58
R	IPL	248	4.76	54	-43	55
R	MTG/ITG	63	4.70	57	-52	-11
L	DLPFC	252	4.63	-33	35	37
L	Postcentral G	46	4.39	-63	-25	37
L/R	Cuneus/precuneus	95	4.04	-6	-79	43

Note: ITG: inferior temporal gyrus; SMA: supplementary motor area; ACC: anterior cingulate cortex; DLPFC: dorsal lateral prefrontal cortex; PCC: posterior cingulate cortex; MFG: middle frontal gyrus; IPL: inferior parietal lobule; MTG: middle temporal gyrus; G: gyrus.